Effect of hard-core repulsion on the structures of a trapped two-dimensional three-boson system

C. G. Bao, Y. Z. He, and G. M. Huang
Department of Physics, Zhongshan University, Guangzhou 510275, People's Republic of China

T. Y. Shi
Department of Physics, Kansas State University, Manhattan, Kansas 66506-2601

(Received 2 August 2001; published 11 January 2002)

A two-dimensional three-boson system interacting with hard-core repulsion and trapped by parabolic confinement has been investigated. Two density functions associated with breathing motion and deformation, respectively, have been defined. Based on these density functions, the wave functions of low-lying states have been analyzed in detailed. The states are found to have explicit geometric features caused by the hard-core repulsion, these features depend strongly on the constraints imposed by symmetry. Striking similarity exists in the density functions, so that breathing bands can be well defined. A classification scheme is thereby proposed.

DOI: 10.1103/PhysRevA.65.022508 PACS number(s): 36.10.−k, 03.75.Fi, 05.30.Jp, 67.40.Db

I. INTRODUCTION

The observation of Bose-Einstein condensation (BEC) in trapped atomic gases has stimulated much theoretical studies on the systems of interacting bosons [1,2]. One of the interesting directions in recent studies is the interplay between the dimensionality and the effect of interaction. The prospects of creating an effectively low-dimensional condensate appear to be very optimistic. For example, the trap containing atomic gases can be made to reach the limit of quasi-two-dimension or quasi-one-dimension, so that interesting effects of dimensionality can also be investigated. A number of theoretical works have been done for BEC in two dimension [3–17] and in one dimension [18–21]. The results from exact diagonalization of the Hamiltonian are compared with those from the mean-field approximation and other approximate methods [16,17,22].

For the two-dimensional case, the studies on rotating Bose-Einstein condensates (BECs) with a weak interaction (approximated by zero-range potential) is interesting [3–16]. The properties of the lowest-energy quantum states with a given nonzero angular momentum, which are referred to as yrast states, have been analyzed by several authors [3–7]. Cooper and Wilkin and Wilken and Gunn revealed the similarities between the quantum states in rotating BECs with the coherence length being larger than the size of the system and in incompressible fractional quantum Hall states [8,9]. They also found the existence of certain angular momentum states of enhanced stability in few-boson systems. Such an angular momentum is called a magic angular momentum.

It is noted that the validity of the zero-range interaction approximation might be questionable if the so-called ''gas parameter,'' which measures the importance of interaction and is defined as na^3 with n being the density of particle and a being the s-wave scattering length, is high [2]. One of the purpose of this paper is to study the properties of trapped boson systems going beyond the zero-range interaction approximation. Since the understanding of particle correlation is a crucial point to understanding any system, a three-boson model system has been chosen to be calculated and analyzed in this paper to expose, in detail, the particle correlation. This analysis would lead to the understanding of the geometric features and the modes of excitation of the system, thereby the quantum states can be classified. Emphasis is placed on the study of the effect of symmetry, which is believed to play an important role but has been of less concern in the previous literatures in BEC.

II. MODEL AND METHOD

Let the three identical bosons of mass m be trapped in a plane by a parabolic confinement with a strength $\hbar\omega_0$. We use $\hbar\omega_0$ and $\sqrt{\hbar/m\omega_0}$ as units of energy and length, respectively, through out the paper. It is assumed that the bosons interact with each other via a short-ranged hard-core repulsion $U\Theta(b-r_{ij})$, where U and b are constants, r_{ij} is the interparticle distance, and $\Theta(x)=1$ if $x\geqslant 0$, or $\Theta(x)=0$ if $x<0$. Let $\vec{r}_i$ be the position vector of the ith boson. Let a set of Jacobi coordinates $\vec{r}$ and $\vec{R}$ be adopted, $\vec{r}=\vec{r}_2-\vec{r}_1$ and $\vec{R}=\vec{r}_3-1/2(\vec{r}_1+\vec{r}_2)$. In the center-of-mass frame, the internal Hamiltonian reads

$$H_I=-\nabla_r^2+\frac{1}{4}r^2-\frac{3}{4}\nabla_R^2+\frac{1}{3}R^2+\sum_{i<j}U\Theta(b-r_{ij}). \quad (1)$$

In order to diagonalize H_I, let us introduce a virtual adjustable single-particle Hamiltonian of harmonic oscillation $-1/2\nabla_s^2+1/2v^2s^2$. Here, $\vec{s}$ is a two-dimensional vector and v is an adjustable parameter. Let $\varphi_{mk}(v\vec{s})$ be an eigenstate of this harmonic oscillation with an eigenenergy $(m+k+1)v$ and an angular momentum $(m-k)\hbar$. Then, the eigenstates of H_I with a given angular momentum L can be expanded as

$$\Psi_L=\mathbf{S}\sum_i C_i\varphi_{mk}\left(\sqrt{\frac{1}{2}}v\vec{r}\right)\varphi_{MK}\left(\sqrt{\frac{2}{3}}v\vec{R}\right). \quad (2)$$

Here, i denotes the set $(mkMK)$, $\mathbf{S}$ is a symmetrizer, $m-k+M-K=L$ is assumed, and v serves as a variational parameter. Ψ_L and the corresponding eigenenergies can be obtained after the diagonalization of H_I. It turns out that, when v is appropriately chosen via a variational procedure, less

than 2000 independent basis functions included in the expansion (2) are sufficient to provide solutions accurate enough for our purpose.

Once the eigenstates Ψ_L have been obtained, a detailed analysis of them will be made. For this purpose, the hyperradius

$$\xi = \sqrt{\frac{1}{2}r^2 + \frac{2}{3}R^2}, \tag{3}$$

and the hyperangle

$$\beta = \frac{2}{3}\left(\frac{R}{\xi}\right)^2, \tag{4}$$

are introduced. Here, β is related to the usually defined hyperangle α by $\beta = \sin^2\alpha$. The domain of β is from 0 to 1, while α is from 0 to $\pi/$. The correlated-densities extracted below using β as the argument is invariant under particle permutations, this is the reason why we use β to replace α. The volume element can be written as

$$\vec{d}r\,\vec{d}R = rR\,dr\,dR\,d\phi_r d\phi_R = \frac{3}{2}\xi^3 d\xi\,d\beta\,d\phi_r d\phi_R. \tag{5}$$

We thus can define the density function associated with the size of the system [23]

$$\rho(\xi) = \int |\Psi_L|^2 \frac{3}{2}\xi^3 d\beta\,d\phi_r d\phi_R \tag{6}$$

fulfilling

$$\int \rho(\xi) d\xi = 1. \tag{7}$$

Instead of using ϕ_r and ϕ_R, we use $\theta = \phi_r - \phi_R$ and ϕ_R as arguments, where θ is the angle between $\vec{r}$ and $\vec{R}$. Then we define the correlated density function associated with deformation

$$\rho(\theta,\beta) = \int |\Psi_L|^2 \frac{3}{2}\xi^3 d\xi\,d\phi_R \tag{8}$$

fulfilling

$$\int \rho(\theta,\beta) d\theta\,d\beta = 1. \tag{9}$$

We shall see that the feature of geometric structure and internal motion can be well understood via the above density functions.

III. RESULTS AND DISCUSSION

All the states have the same L constitute a L series. Let L_i denotes the ith state of a L series. The energies of the low-lying L_i states with $U=200$ and $b=0.1$ are listed in Table I. Where the ground state has an energy $E(0_1)=2.847$. If the hard-core repulsion is removed, we would have $E(0_1)=2$.

TABLE I. The eigenenergies of the L_i states with $U=200$ and $b=0.1$.

	$i=1$	$i=2$	$i=3$	$i=4$
$L=0$	2.847	4.899	6.222	6.942
$L=1$	5.713	7.165	7.737	
$L=2$	4.511	6.535	7.999	
$L=3$	5.220	7.228	7.631	
$L=4$	6.370	8.192	8.364	
$L=5$	7.294	9.301	9.483	
$L=6$	8.000	8.338	10.001	

So, the additional 0.847 arises from the hard-core repulsion. When the center-of-mass (c.m.) motion is taken into account, it has been found that for some systems the lowest-energy state of any L series is the one where the angular momentum is all carried by the c.m. motion [10]. This finding does not fit the present system. For example, we know from the table that the energy difference of the 2_1 and 0_1 states is 1.664. When the c.m. motion is taken into account and if the angular momentum of the 2_1 state arises from the c.m. motion, then the energy difference would be 2. Therefore, the lowest $L=2$ state of our case cannot have the c.m. motion excited. Similarly, we can see that the lowest $L=3$ and 6 states cannot have their c.m. motion excited.

It was found by Pitaevskii and Rosch [24] that two-dimensional bosonic systems with zero-range interactions display a breathing mode arising from the $SO(2,1)$ symmetry, the energy difference of adjacent breathing levels is $2\hbar\omega_0$. Although the hard-core interaction with a finite range is used in this paper to replace the zero-range interaction, the feature of the $2\hbar\omega_0$ spacing remains in the spectrum. For an example, from the table we found that $E(0_2)$-$E(0_1)$ $=2.052$ and $E(0_4)$-$E(0_2)=2.043$. Thus, the 0_1, 0_2, and 0_4 might be the members of a breathing band. Furthermore, we have $E(0_5)$-$E(0_3)=2.012$, thus they might be the members of another breathing band. We shall give further evidence on the existence of these bands. The $2\hbar\omega_0$ spacing appears also in $L\neq 0$ states. For examples, the $E(L_3)$-$E(L_1)$ with $L=1$, 4, and 6, and the $E(L_2)$-$E(L_1)$ with $L=2$, 3, and 5 are all very close to 2 as shown in the table. Thus, the breathing mode existing in the systems with zero-range interactions might also exist in our system. This is an interesting point, it implies that the hard core does not yield very different results than the zero-range interaction. In fact, the energy spectra of these two types of interaction are similar. For examples, when the interaction $U\Theta(b-r_{ij})$ is replaced by $\eta/2\delta(x_i - x_j)\delta(y_i-y_j)$ and if the strength $\eta=1.2$, then the calculated energies of 0_1 to 0_5 are 2.227, 4.231, 6.059, 6.241, and 8.076, respectively. Thus, just as the hard core, the 0_1 to 0_5 states are divided into two bands. The first, second, and fourth states belong to the lowest band, while the third and fifth belong to a higher band.

Let us study the wave functions. It is noted that $\beta=0$, 1/4, 1/2, 3/4 and 1 correspond to $R/r=0$, 1/2, $\sqrt{3}/2$, 3/2, and ∞, respectively. Thus, in the $\theta-\beta$ plane, the point (θ,β) $=(\pi/2,1/2)$ is associated with an equilateral triangle (ET),

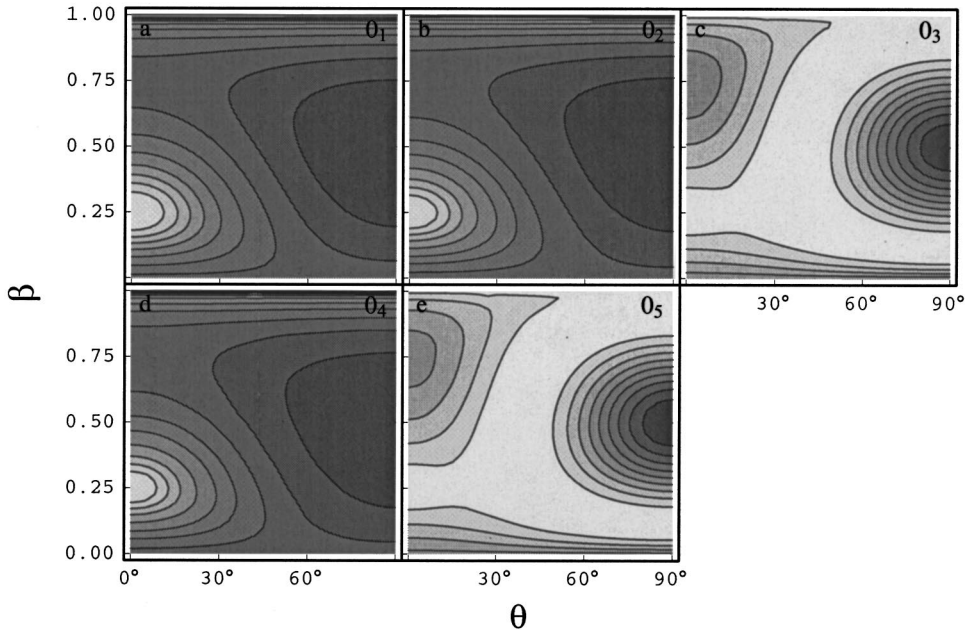

FIG. 1. Contour diagrams of $\rho(\theta, \beta)$ of the $L=0$ states with the hard-core interaction. $U=200$ and $b=0.1$ are assumed, The darker area has a larger $\rho(\theta, \beta)$. The contours are symmetric with respect to $\theta=90°$.

the points (0, 3/4) and $(\theta, 0)$ are both associated with a cigar shape with two particles located at the two ends and one right at the middle (denoted as CG1), the points (0, 1/4) and $(\theta, 1)$ are both associated with another cigar shape with two particles located at the same end while the other one at the opposite end (denoted as CG2). With this in mind, let us first observe the $\rho(\theta, \beta)$ of $L=0$ states as plotted in Fig. 1. Figs. 1(a), 1(b), and 1(d) are strikingly similar, they all have a peak at an ET and the wave function extends smoothly to the CG1. Therefore, the geometric features of the 0_1, 0_2, and 0_4 states are the same, they all are a mixture of the ET and CG1, the former is more important. The $\rho(\xi)$ of them are given in Fig. 2. They have one, two, and three peaks, respectively. Therefore, the breathing mode (the contraction and extension of the size) is not excited in 0_1, but is excited in 0_2 with one node, and is more fiercely excited in 0_4 with two nodes. Since these states are highly similar in $\rho(\theta, \beta)$, the formation of the suggested breathing band is confirmed. Since this band is based on the mixture of ET and CG1, it is called an (ET $+$CG1) band.

It is noted that the $\rho(\xi)$ of the 0_1 is peaked at $\xi=1.52$, the associated side length of the most probable ET is also 1.52, therefore, the average particle-particle separation is much larger than the radius b of the hard core. This is a very interesting point that a well-defined geometric structure can be caused by a hard core even the radius of the core is much smaller than the average interparticle distance. The two peaks of the $\rho(\xi)$ of the 0_2 is located at $\xi=1.1$ and 2.5, respectively. It implies that the amplitude of the breathing is quite large. For higher members of the (ET$+$CG1) band, the amplitude is even larger.

The $\rho(\theta, \beta)$ of the 0_3 and 0_5 states are given in Figs. 1(c) and 1(e), they are also strikingly similar to each other but different from those of the (ET$+$CG1) band. They all have a sharp peak at an ET, and two lower peaks at (0, 3/4) and $(\theta, 0)$ both associated with the cigar-shape CG1 but having different permutations of particles at the shape. Since $\rho(\theta, \beta)$ is invariant with respect to particle permutation, the two lower peaks have exactly the same height. The trajectory from the sharp peak $(\pi/2, 1/2)$ to the lower peak $(\pi/2, 0)$ is associated with a contraction of the height of an isosceles triangle and/or an extension of the base. This is called a hinge mode of oscillation [25] that transforms an ET to an CG1, and vice versa. Since there is a node lying along the trajectory, the hinge mode has been excited. The trajectory from $(\pi/2, 1/2)$ to (0, 3/4) is mainly associated with a swing of $\vec{R}$ (a variation of θ). This is called a swing mode of oscillation [25] that transforms also an ET to an CG1, and vice versa. A node is also contained in this mode, so the swing mode is also excited. The $\rho(\xi)$ of 0_3 and 0_5 shown in Fig. 2 demonstrate that the breathing mode is not excited in 0_3 but excited in 0_5. Since their $\rho(\theta, \beta)$ are highly similar, they form another breathing band based also on the mixture of the ET and CG1

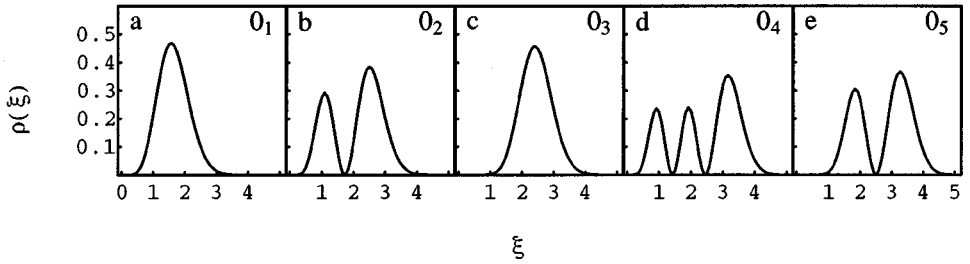

FIG. 2. $\rho(\xi)$ of the $L=0$ states. $U=200$ and $b=0.1$ are assumed.

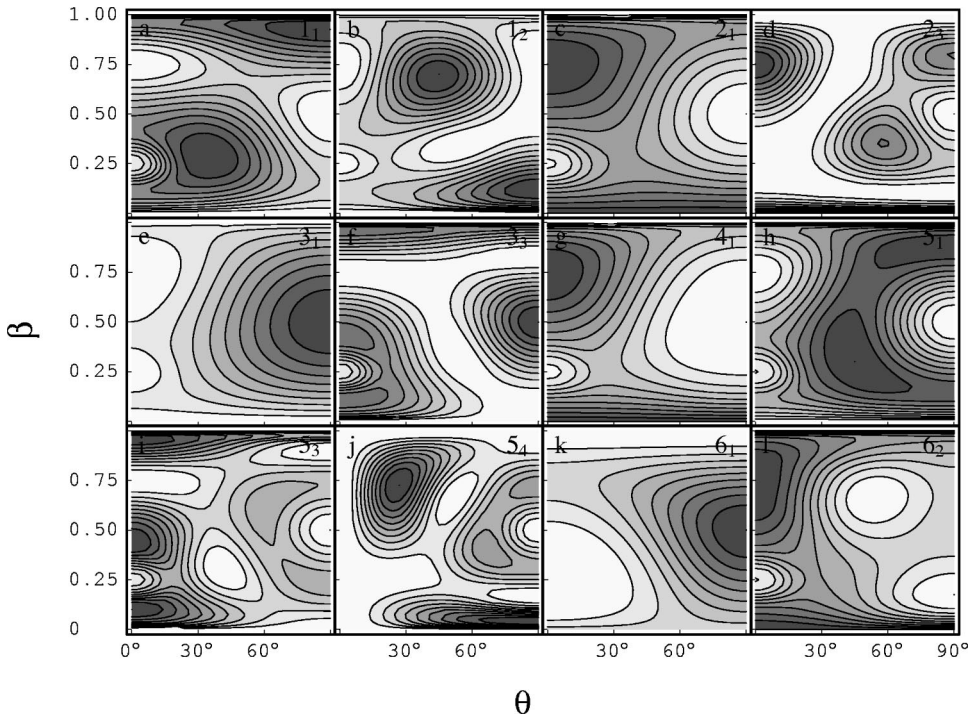

FIG. 3. Contour diagrams of $\rho(\theta, \beta)$ of the $L \neq 0$ states. $U = 200$ and $b = 0.1$ are assumed.

but with the hinge mode and swing mode excited. This band is called a (ET+CG1)* band. In this band, the excited hinge mode and swing mode coexist with the breathing mode.

It is noted that, for $L \neq 0$ states, the ET and/or CG1 may be prohibited by symmetry. When the particles form an ET, a rotation by $2\pi/3$ about the c.m. is equivalent to a cyclic permutation of particles. The rotation would cause the appearance of a factor $e^{-i2\pi L/3}$ in the wave functions, while the permutation would cause no effect in bosonic systems. Thus, the ET is allowed only if $\{L \equiv 0 \bmod 3\}$, otherwise the wave function has to be zero at the ET. When the particles form a CG1, a rotation by π is equivalent to an interchange of the two particles at the ends of the CG1. The former would induce a factor $e^{-i\pi L}$, while the latter would cause no effect as before. Thus, the CG1 is allowed only if L is even.

For $L=1$ states, both the ET and CG1 are prohibited. Since the prohibition of a shape implies the appearance of a node in the wave function at the shape, since the existence of a node implies an excitation of motion, the kinetic energy thereby increases. For these reasons, the 1_1 state is quite high in energy as shown in Table I, it is even higher than the 2_1 and 3_1 states. The $\rho(\theta, \beta)$ of the 1_1 state is plotted in Fig. 3(a), there are three nodes associated with the prohibition of the ET and CG1 (due to the symmetry constraints), and the prohibition of the CG2 (due to the hard core). On the other hand, there are two peaks, both are associated with a very sharp isosceles triangle (close to a CG2). Since the $\rho(\theta, \beta)$ is invariant with respect to particle permutation, these two peaks have exactly the same height. Furthermore, the glaring similarity found in the $L=0$ states emerges also in $L \neq 0$ states. The $\rho(\theta, \beta)$ of the 1_3 state is found to be strikingly similar to the one of the 1_1 state, and the $\rho(\xi)$ of the 1_1 and 1_3 states contain one and two peaks, respectively. Thus, there is a breathing band based on the sharp triangle, it is called a sharp-triangle band. The 1_2 and 1_4 states have strikingly similar $\rho(\theta, \beta)$ as shown in Fig. 3(b), where the peaks are peaked at a very flat isosceles triangle. Furthermore, the $\rho(\xi)$ of the 1_2 and 1_4 states are found to contain one and two peaks, respectively. Thus, they form the flat-triangle band.

While the ET is not allowed in $L=2$ states, the CG1 is allowed. Thus, one would expect that $L=2$ states would prefer the cigar shape. This is confirmed as shown in Fig. 3(c), where peaks are located at the CG1. Based on the CG1, a breathing band with the members $2_1, 2_2, 2_4 \ldots$ is found (the CG1 band). The 2_3 state is found to be a mixture of a CG1 and a sharp isosceles triangle as shown in Fig. 3(d).

While the CG1 is not allowed in $L=3$ states, the ET is allowed. Thus, one would expect that $L=3$ states would prefer the ET but deny the CG1. In fact, the main band (the lowest band) of $L=3$ states is an ET band with members $3_1, 3_2, 3_5 \ldots$ They have very similar $\rho(\theta, \beta)$ as shown in Fig. 3(e). In the ET band, the wave functions do not extend to the CG1, thus, the ET shape is well defined. The 3_3 state is found to be a mixture of an ET and a collinear structure with the third particle oscillating back and forth around the center of a cigar shape with a node at the center as shown in Fig. 3(f).

The $L=4$ and 2 states are similarly constrained by symmetry. The CG1 band found in $L=2$ states exists also in $L=4$ states. The 4_1 and 4_3 are members of this band as shown in Fig. 3(g). On the other hand, the 4_2 and 4_5 are found to be the members of a sharp-triangle band. Incidentally, Figs. 3(c) and 3(g) are very similar. Thus, *similarity exists not only among the states with the same L, but also among the states with different L but similarly constrained by symmetry*.

The $L=5$ and 1 states are similarly constrained by symmetry. Both the sharp-triangle band and the flat-triangle band found in $L=1$ states exist also in $L=5$ states. The members of these two bands are $5_1, 5_2, \ldots,$ and $5_4, \ldots,$ respectively, as

TABLE II. The breathing bands.

Bands	Members	Examples of $\rho(\theta,\beta)$
(ET+CG1)	$0_1, 0_2, 0_4, \cdots 6_1, 6_3 \cdots$	Figs. 2(a), 2(b), 2(d), 3(k)
(ET+CG1)*	$0_3, 0_5, \cdots 6_2, 6_5, \cdots$	Figs. 2(c), 2(e), 3(l)
Sharp-triangle	$1_1, 1_3, \cdots 4_2, 4_5, \cdots 5_1, 5_2, \cdots$	Figs. 3(a), 3(h)
Flat-triangle	$1_2, 1_4, \cdots 5_4, \cdots$	Figs. 3(b), 3(j)
CG1	$2_1, 2_2, 2_4, 4_1, 4_3, \cdots$	Figs. 3(c), 3(g)
ET	$3_1, 3_2, 3_5, \cdots$	Fig. 3(e)

shown in Figs. 3(h) and 3(j). The 5_3 state is collinear and is dominated by collinear oscillation with a node at the CG1 as shown in Fig. 3(i). This state can be called a CG* state (here, the star implies the excited oscillation existing in the cigar shape). Although higher states have not been analyzed, it is believed that, based on the finding of Pitaevskii and Rosch [24], a CG* band characterized by the excited collinear oscillation would exist. Since the collinear structure has a larger moment of inertia and therefore can reduce the rotation energy, it will appear quite often in the low-lying states with a larger L.

Similar to the $L=0$ states, both the ET and CG1 are allowed in $L=6$ states. The (ET+CG1) band and the (ET+CG1)* band found in $L=0$ states exist also in $L=6$ states. The members of the (ET+CG1) band are $6_1, 6_3, \ldots$, as shown in Fig. 3(k). The members of the (ET+CG1)* band are $6_2, 6_5, \ldots$, as shown in Fig. 3(l). It is recalled that in the (ET+CG1)* band of $L=0$ states, the peak at the ET is higher. However, in the (ET+CG1)* band of $L=6$ states, the peak at the ET is small. Evidently, when L gets larger and larger, collinear structures will become more preferred.

The breathing bands are summarized in Table II. When we change the radius of the core, while the repulsive core remains to be hard. The above findings remain true in the qualitative aspect. For example, if $U=1000$ and $b=0.03$, the $\rho(\theta, \beta)$ of some selected states are plotted in Fig. 4. These contour diagrams are very similar to the corresponding diagrams in Figs. 1 and 3.

Since only the lower states have been investigated in this paper, in addition to the bands listed in Table II, more bands higher in energy would also exist. It was shown in Table II that states distinct in L may belong to the same breathing band, they are similar in $\rho(\theta, \beta)$ and may have the same number of peaks in $\rho(\xi)$. For example, the 0_1 and 6_1 both belonging to the (ET+CG1) band are qualitatively similar in $\rho(\theta, \beta)$ [refer to Figs. 1(a) and 3(k)], and both have a peak in $\rho(\xi)$. The former is peaked at $\xi=1.52$, while the latter is peaked at $\xi=2.74$, thus, the 6_1 has a much bigger size. Since they are qualitatively similar in $\rho(\theta, \beta)$ and $\rho(\xi)$, they can be further grouped in a rotation band denoted as the $(\mathrm{ET+CG1})_0$ band, where the subscript 0 denotes that the breathing oscillation contains zero node. Similarly, the 0_2 and 6_3 form a rotation band, the $(\mathrm{ET+CG1})_1$ band, containing a node in the breathing oscillation; the 2_1 and 4_1 form a rotation band, the $(\mathrm{CG1})_0$ band, containing zero node in the breathing oscillation, etc.

It is noted that the ET and CG1 are strictly constrained by symmetry, therefore, the members of the rotation band based on these shapes are strictly selected by symmetry and can be more or less predicted. For an example, the members of the

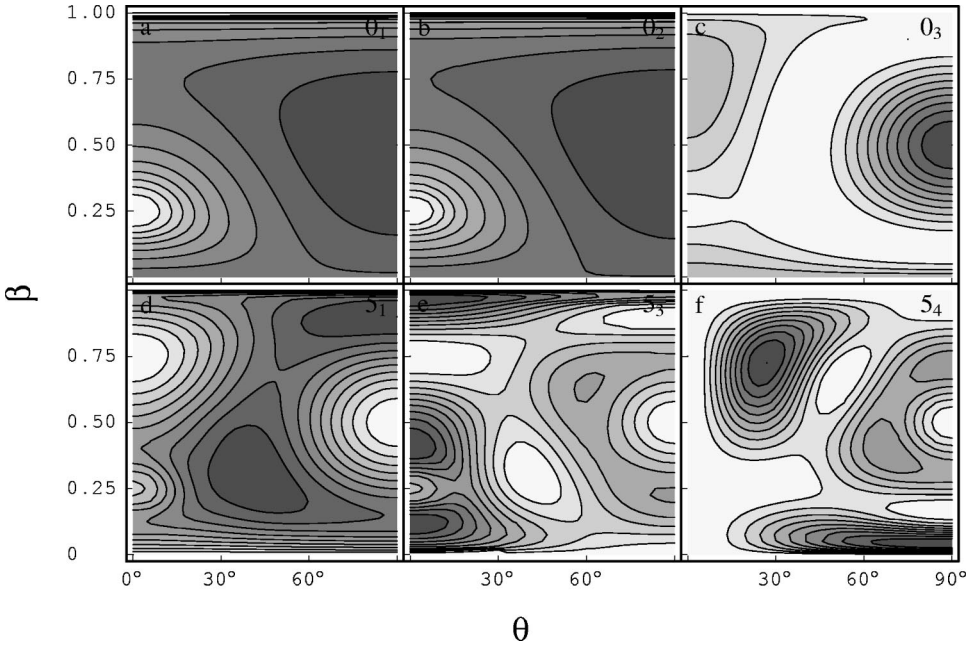

FIG. 4. Contour diagrams of $\rho(\theta, \beta)$ of the $L=0$ states. $U=1000$ and $b=0.03$ are assumed.

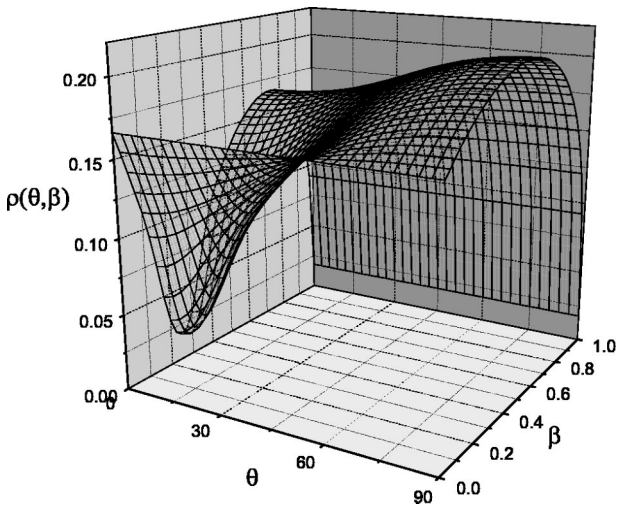

FIG. 5. 3D surface diagrams of $\rho(\theta, \beta)$ of the $L=0$ states with the zero-range interaction. $\eta=12$ is assumed.

$(\mathrm{ET}+\mathrm{CG1})_0$ band should contain only the both ET- and CG1-accessible states. Thus, they are expected to be the $0_1,6_1,12_1,18_1,\ldots,$ states; while the members of the $(\mathrm{CG1})_0$ band should contain the ET-inaccessible and CG1-accessible states $2_1,4_1,8_1,10_1,\ldots,$. On the other hand, the sharp triangle and flat triangle are not constrained by symmetry, thus the members of the associated bands are difficult to be foreseen. For an example, the $L=4$ and 5 states are differently constrained by symmetry, but they both are found in the sharp-triangle band (refer to Table II).

For a comparison of the effects of the two types of interaction on wave functions, the results of $\rho(\theta, \beta)$ of the 0_1 state with a zero-range interaction $\eta/2\delta(x_i-x_j)\delta(y_i-y_j)$ and with $\eta=12$ are plotted in Fig. 5. It is shown that the results found in Fig. 5 are qualitatively very similar to those in Fig. 1(a). Thus, the zero-range interaction is a good approximation to the hard-core interaction. It was shown that the range of the $\rho(\theta, \beta)$ in Fig. 5 is from 0.025 to 0.20. If η is reduced to 1.2 and 0.12, the figure would remain nearly unchanged if the Z axis is rescaled and the range is from 0.12–0.17, and from 0.155–0.160, respectively. Thus, when η is greatly reduced, the distribution with respect to θ and β is close to be uniform.

IV. SUMMARY

We have calculated numerically the low-lying eigenstates and energies for an interacting two-dimensional (2D) three-boson system. A hard-core potential between bosons is assumed. We reach the following conclusions.

(i) The density functions $\rho(\xi)$ and $\rho(\theta, \beta)$ defined in this paper are found to be very useful in the analysis of wave functions, the structures of low-lying states can be therefore well understood. Very detailed information on the eigenstates of the two-dimensional trapped three-boson system with hard-core repulsion has been obtained. To the knowledge of the authors, the correlated density $\rho(\theta, \beta)$ has not yet been calculated before. It is worthy to introduce this function in the investigation of other three-body systems, including three-dimensional systems. In the cases of three-dimensional systems, $\rho(\theta, \beta)$ should be generalized to $\rho_Q(\theta,\beta)$ fulfilling

$$\sum_Q \int \rho_Q(\theta,\beta)d\theta\, d\beta = 1, \tag{10}$$

where Q is the component of L along the third axis of a body frame [26].

(ii) It was found that the hard core does not yield very different results than the zero-range interaction. They have similar spectra. Specifically, the breathing bands existing in the systems with zero-range interactions are found to exist also in the systems with hard-core repulsion. Furthermore, their wave functions are also one-to-one similar.

(iii) It is interesting to see that very clear geometric structures can be induced by the hard-core repulsion. This is true even if the radius of the core is very small, if the core is hard enough, and even in the case of zero-range interactions, if η is large enough. Striking similarity in $\rho(\theta, \beta)$ was found to exist among specific states, this fact is expected from the SO(2, 1) symmetry and leads to the formation of breathing bands. The internal structures of the bands can be understood by observing $\rho(\theta, \beta)$. The low-lying states can be classified into several bands. The character of each band and the members of the band have been clarified.

(iv) The members of a breathing band may have different L, thus they can be further classified into rotation bands, e.g., the $(\mathrm{ET}+\mathrm{CG1})_1$ band. This leads to a complete classification scheme. The angular momenta of a rotation band is found to jump from a value to another separate value [e.g., $L=0,6,12,...,$ in the $(\mathrm{ET}+\mathrm{CG1})_0$ band] due to the symmetry constraints, this is a noticeable feature.

(v) The effect of symmetry is found to be great, in particular for the low-lying states. The feature of $\rho(\theta, \beta)$ depends strongly on the ET and CG1 accessibility, which are determined by symmetry. In fact, the structures of low-lying states can be objectively classified according to the ET and CG1 accessibility, thereby the classification scheme was proposed. The states constrained in the same way by symmetry have similar structures (e.g., the $L=0$ and 6 states, or the $L=1$ and 5 states), these structures can be more or less predicted.

(vi) The eigenenergies of the both ET-accessible and CG1-accessible L_1 states, namely, the $0_1,6_1,\ldots,$ states, are found to be relatively lower. They are the first candidates of the ground state in a rotating bosonic system. The ET-accessible but CG1-inaccessible L_1 states, namely the $3_1,9_1,\ldots,$ states, are the second candidates. The idea of accessibility might be generalized to explain the stability of states of a general bosonic system, and therefore might explain the magic numbers found in rotating bosonic systems. This point deserves a deeper study.

It is planned to extend the above investigation to the systems containing more bosons.

ACKNOWLEDGMENTS

This work is supported by the NSFC under Grant Nos. 90103028 and 10174098. T.Y.S. is supported in part by Chemical Sciences, Geosciences and Biosciences Division, Office of Basic Energy Sciences, Office of Science, U.S. Department of Energy.

[1] F. Dalfovo, S. Giorgini, L. P. Pitaevskii, and S. Stringari, Rev. Mod. Phys. **71**, 463 (1999).
[2] A. J. Leggert, Rev. Mod. Phys. **73**, 307 (2001).
[3] B. Mottelson, Phys. Rev. Lett. **83**, 2695 (1999).
[4] G. F. Bertsch and T. Papenbrock, Phys. Rev. Lett. **83**, 5412 (1999).
[5] G. M. Kavoulakis, B. Mottelson, and C. J. Pethick, Phys. Rev. A **62**, 063605 (2000).
[6] G. M. Kavoulakis, B. Mottelson, and S. M. Reimann, Phys. Rev. A **63**, 055602 (2001).
[7] T. Nakajima and M. Ueda, Phys. Rev. A **63**, 043610 (2001).
[8] N. R. Cooper and N. K. Wilkin, Phys. Rev. B **60**, R16279 (1999).
[9] N. K. Wilkin and J. M. F. Gunn, Phys. Rev. Lett. **84**, 6 (2000).
[10] N. K. Wilkin, J. M. F. Gunn, and R. A. Smith, Phys. Rev. Lett. **80**, 2265 (1998).
[11] R. A. Smith and N. K. Wilkin, Phys. Rev. A **62**, 061602(R) (2000).
[12] W.-J. Huang, Phys. Rev. A **63**, 015602 (2000).
[13] T. Papenbrock and G. F. Bertsch, Phys. Rev. A **63**, 023616 (2001).
[14] A. D. Jackson, G. M. Kavoulakis, B. Mottelson, and S. M. Reimann, Phys. Rev. Lett. **86**, 945 (2001).
[15] B. Paredes, P. Fedichev, J. I. Cirac, and P. Zoller, Phys. Rev. Lett. **87**, 010402 (2001).
[16] T. Haugset and H. Haugerud, Phys. Rev. A **57**, 3809 (1998).
[17] M. A. H. Ahsan and N. Kumar, Phys. Rev. A **64**, 013608 (2001).
[18] W. Ketterle and N. J. van Druten, Phys. Rev. A **54**, 656 (1996).
[19] B. Tanatar and K. Erkan, Phys. Rev. A **62**, 053601 (2000).
[20] M. D. Girardeau and E. M. Wright, Phys. Rev. Lett. **84**, 5239 (2000); **94**, 5691 (2000).
[21] M. D. Girardeau, E. M. Wright, and J. M. Triscari, Phys. Rev. A **63**, 033601 (2001).
[22] T. Papenbrock and G. F. Bertsch, Phys. Rev. A **58**, 4854 (1998).
[23] Y. Z. He and C. G. Bao, J. Phys. B **33**, 1641 (2001).
[24] L. P. Pitaevskii and A. Rosch, Phys. Rev. A **55**, R853 (1997).
[25] G. Herzberg, *Molecular Spectra and Molecular Structure* (Krieger, Princeton, NJ, 1945).
[26] C. G. Bao, W. F. Xie, and W. Y. Ruan, Few-Body Syst. **22**, 135 (1997).